PERGAMON

Journal of Structural Geology 21 (1999) 695–702

JOURNAL OF STRUCTURAL GEOLOGY

Kinematic modelling of extensional fault-propagation folding

Stuart Hardy[a,*], Ken McClay[b]

[a]Basin and Stratigraphic Studies Group, Department of Earth Sciences, The University of Manchester, Manchester M13 9PL, UK
[b]Fault Dynamics Research Group, Department of Geology, Royal Holloway University of London, Egham Hill, Egham, Surrey, TW20 0EX, UK

Received 9 February 1998; accepted 17 March 1999

Abstract

Many studies have shown that in extensional basins discrete faulting at depth is commonly linked to more distributed deformation, in particular folding, at higher levels. Such extensional fault-propagation folds are particularly common where there is a distinct mechanical contrast between faulted basement and sedimentary cover. Outcrop and analogue modelling studies indicate that such folds form as upward widening zones of distributed deformation (monoclines) above discrete faults at depth. With increasing displacement (strain) the folds are cut by faults as they propagate upwards into the cover. To date, however, there has been little investigation into the kinematics of linked basement faulting and extensional fault-propagation folding. Here we present a two-dimensional kinematic model of linked basement faulting and fault-propagation folding which is based upon trishear. The model allows investigation of the influence of shear zone geometry and the rate of fault propagation upon the style of folds and the strains associated with them. The evolution of linked basement faulting and folding predicted by the model is compared in detail to that observed in an analogue model. The kinematic model reproduces well many of the features seen both in the analogue model and reported from outcrop and seismic studies.

1. Introduction

Extensional fault-propagation folds form above steeply dipping normal faults (Fig. 1a and b) typically, though not exclusively, where there is a distinct mechanical contrast between basement and sedimentary cover or a ductile unit overlies the basement and acts to decouple the basement and overlying sediments (see Withjack et al., 1990; Stewart et al., 1996; Gawthorpe et al., 1997). They have been recognized from many areas of the world, e.g. the Rhine Graben (Laubscher, 1982), the Gulf of Suez (Gawthorpe et al., 1997) and the North Sea (Withjack et al., 1988), and have received much attention due to the frequent occurrence of hydrocarbons associated with the folds themselves and the underlying fault blocks. Evidence from well-exposed folds with preserved growth strata (Gawthorpe et al., 1997) and from analogue (Withjack et al., 1990) and numerical modelling (Patton and Fletcher, 1995) has indicated that extensional fault-propagation folds form as upward widening zones of distributed deformation (monoclines) above discrete faults at depth. Field studies indicate that a variety of mechanisms are responsible for the distributed deformation including ductile flow, bedding slip, rigid rotation and small extensional and thrust faults (e.g. Gawthorpe et al., 1997). Analogue modelling studies have shown that with increasing displacement (strain) the overlying fold is cut by the fault as it propagates upwards into the cover. Where a faulted rigid basement is involved in the deformation the folds are often called forced folds (Withjack et al., 1990), while it has been suggested by Schlische (1995) that the drag folds of some workers are in fact breached extensional fault-propagation folds. While these aspects of extensional fault-propagation folds are reasonably well understood (e.g. Schlische, 1995; Janecke et al., 1998), the kinematics of the linkage between deeper faulting and shallower distributed deformation is not. Here we present a two-dimensional kinematic model of linked

* Corresponding author.
E-mail address: shardy@fs1.ge.man.ac.uk (S. Hardy)

0191-8141/99/$ - see front matter
PII: S0191-8141(99)00072-3

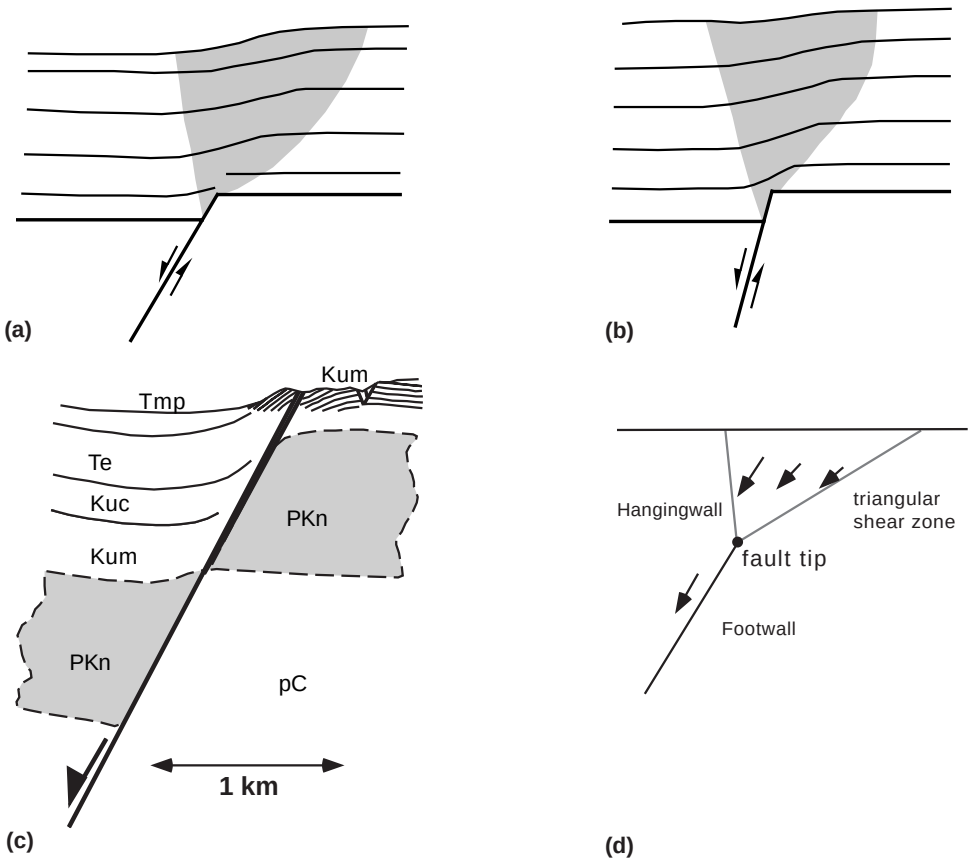

Fig. 1. (a), (b) Cross-sections from analogue (clay) models illustrating extensional fault-propagation folds—highlighted in gray shading (redrawn from Withjack et al., 1990), (c) outcrop of a breached fold from the Gulf of Suez (redrawn from Withjack et al., 1990; pC—Precambrian, PKn—Carboniferous, Upper Cretaceous, Kum—Upper Cretaceous, Kuc—Upper Cretaceous, Paleocene, Te—Eocene, Tmp—Miocene, Pliocene, Holocene), (d) schematic illustration of the kinematic model of fault-propagation folding used in this paper—see text for further details.

basement faulting and extensional fault-propagation folding which builds upon an earlier adaptation of trishear (Hardy and Ford, 1997), and use this model to investigate the influence of shear zone geometry and the rate of fault propagation on both the geometry of, and the strain variation within, extensional fault-propagation folds. The predictions of the model are compared to a laboratory analogue model and field examples. The model is shown to account well for many of the features seen both in outcrop examples and analogue modelling studies.

2. Two-dimensional kinematic model

Field and experimental studies (Fig. 1a, b, c) indicate that distinct faulting at depth is often expressed at shallower levels by upward widening zones of distributed deformation (generally monoclinal) in which there is no distinct throughgoing fault. These broadly triangular zones of deformation narrow downsection and die out near the fault tip. As discussed previously with reference to compressional structures (Hardy and Ford, 1997), this is very similar geometrically to the trishear model (Erslev, 1991) where a triangular zone of distributed deformation (shearing) is attached to a fault tip (Fig. 1d) and can be either hanging wall- or footwall-fixed. Within the shear zone both the magnitude and direction of the displacement vector vary, with slip tending to zero towards the footwall. Hardy and Ford (1997) used the trishear model in a compressional setting to address a more general situation in

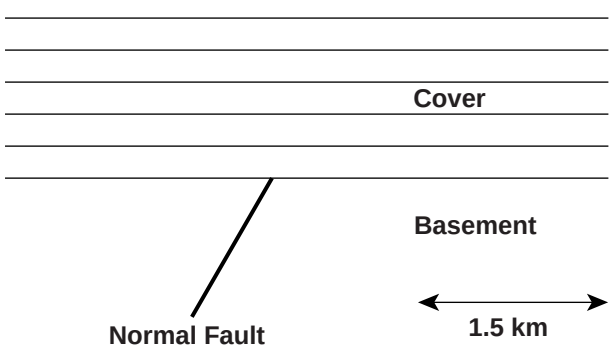

Fig. 2. Initial configuration of the models discussed in this paper. A distinct normal fault at depth is overlain by a 1.5 km thick cover stratigraphy. No vertical exaggeration.

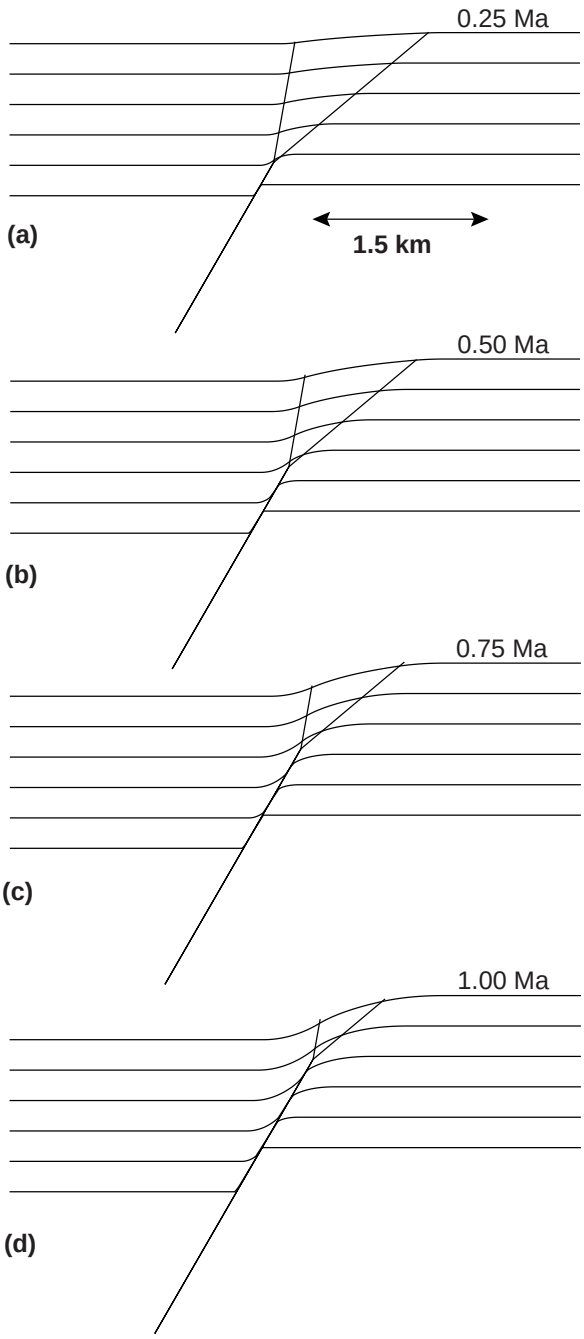

Fig. 3. Sequential evolution of a model having a 60° normal fault with a trishear zone with a 40° apical angle attached to its tip. Slip parallel to the normal fault is 0.5 m/ka over a total run time of 1 Ma. The fault propagates into the cover stratigraphy at twice the slip rate. Model is shown after (a) 0.25, (b) 0.50, (c) 0.75 and (d) 1.00 Ma. Both the fault and the position of the triangular shear zone at each stage of development are indicated. No vertical exaggeration.

which the zone of distributed deformation is attached to a fault tip which propagates up through a sedimentary section at a rate which is independent of the slip rate. Fault propagation from a flat décollement and growth strata were also incorporated into the model. The detailed derivations of the velocity description of deformation for the trishear model (the kinematics) and its implementation are given in Hardy and Ford (1997).

Here we apply this kinematic model to the problem of extensional fault-propagation folding where the zone of distributed deformation is assumed to be fixed to a fault tip which originally lies at the basement–cover interface (Fig. 2). Within the basement we assume that there exists initially a discrete fault whereas in the cover there is no faulting. As slip occurs on the basement fault the overlying strata are deformed within the shear zone. The nature and location of deformation during fault slip are controlled by two parameters—the apical angle of the shear zone and the fault propagation to slip ratio (p/s). The apical angle of the shear zone controls how widely deformation is distributed above the fault tip, while p/s controls how rapidly the fault tip (and its associated zone of deformation) propagates upwards through the rock mass. This model is used here to investigate the influence of shear zone geometry and rates of fault propagation on both the style of, and strain within, extensional fault-propagation folds. The deformation is monitored with respect to the initially flat-lying, constant-thickness beds and also through the use of initially circular strain markers. The detailed modelling methodology is given in Hardy and Ford (1997).

3. Modelling of extensional fault-propagation fold geometries

In this section some examples of the structural relationships that are produced by the kinematic model of extensional fault-propagation folding described above are presented. In all the models a normal fault cutting basement at 60° will be used together with an initial unfaulted cover stratigraphy 1.5 km thick (Fig. 2). Models were run for a total of 1 Ma using a slip rate of 0.5 m/ka parallel to the fault. In this section the influence of two parameters on the geometries of the structures developed will be investigated: the shear zone apex angle and the fault-propagation to slip (p/s) ratio.

Fig. 3 shows the sequential development of the basic model described above using a shear zone apex angle of 40° and p/s of 2.0. This model will be used as the standard model against which the other models will be compared. The development of the structure with increasing slip (displacement) is shown after 0.25, 0.50, 0.75 and 1.00 Ma. It can be seen that an upward-widening monocline forms above the discrete fault in the basement with beds showing thinning in anticlinal areas. Through time the limb of the monocline steepens with the final dip reaching approximately 25°. As the fault propagates up-section (at a rate controlled by

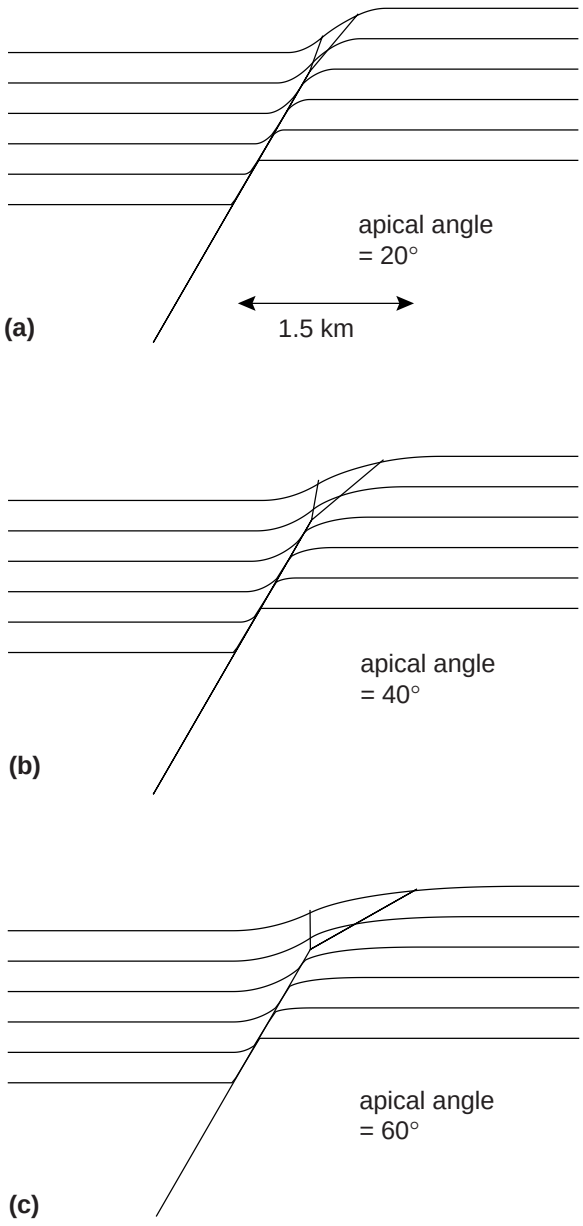

Fig. 4. Model results illustrating the effect of different apical angles of the shear zone on fold geometries. Apical angles of (a) 20°, (b) 40° and (c) 60°. Total run time is 1 Ma. All other model parameters are as in Fig. 3.

p/s) it can be seen to cut the overlying fold producing hanging wall-synclines and footwall-anticlines on either side of the fault plane. These are remnants of the breached monocline and are not the result of 'drag' adjacent to the fault (cf. Fig. 1c). At the end of the model run (1 Ma) only a small part of the monocline remains uncut by the fault.

In Fig. 4 the final results of the basic model described above with shear zone apex angles of 20°, 40° and 60° are shown. All other model parameters are identical to those used in Fig. 3. These results show that with decreasing apical angle of the shear zone the monocline decreases in wavelength but becomes steeper. As a result, the deformation within the shear zone is more intense and localized, resulting in more thinning of beds. It is clear that as the apical angle of the shear zone tends to zero deformation takes place in an increasingly narrow and intense zone ahead of the fault tip. This results in hanging wall-synclines and footwall-anticlines that are restricted to a narrow zone immediately adjacent to the fault plane.

In Fig. 5 the effects of variations in p/s on the basic model are shown. The basic model of Fig. 3 was run with p/s of 1, 2 and 4; all other parameters were unchanged. It can be seen that with increasing p/s values the fault-propagation folds are cut increasingly early in their development by the propagating fault. Thus, in the model with a p/s of 4, the fault has cut through all of the cover stratigraphy and shows only a throughgoing fault with no active zone of distributed deformation. This structure therefore has undergone a two-stage evolution—an early stage of coupled faulting and distributed deformation followed by a later stage when the fault propagated through the entire cover stratigraphy (and broke the surface) and no zone of distributed deformation was present. Precisely this type of evolution has recently been reported from detailed analysis of growth strata associated with extensional faults in the Gulf of Suez (Gawthorpe et al., 1997).

In Fig. 6 the nature of strains in the hanging wall and footwall in the immediate vicinity of the fault plane for the models in Fig. 5 are shown. Initially circular strain markers were included in these model runs to assess the strain. These strain markers initially have a radius of 50 m and thus represent the strain at scales larger than typical outcrops. What can be seen is that while in all of the models the width of the monocline is broadly similar, the nature of the deformation within it is quite different. Low p/s values can be seen to lead to greater extensional strains in the fold ahead of the fault tip before being cut (e.g. Fig. 6a) leading to more ductile fold profiles. In contrast, with higher p/s values (e.g. Fig. 6c) folds undergo a lesser amount of strain before being cut by the propagating fault.

4. Comparison with an analogue model

Here we test the applicability of our model by comparing it to a well-constrained analogue (clay) model described in detail by Withjack et al. (1990). We use an analogue model for comparative purposes as it provides us with a temporal picture of the evolution of a fault-propagation fold—a feature rarely observable in natural examples except when excellent growth strata are preserved. The analogue model is a single-layer clay model above a 75° normal fault. The development of the structure is shown after 1, 2 and 3 cm of displa-

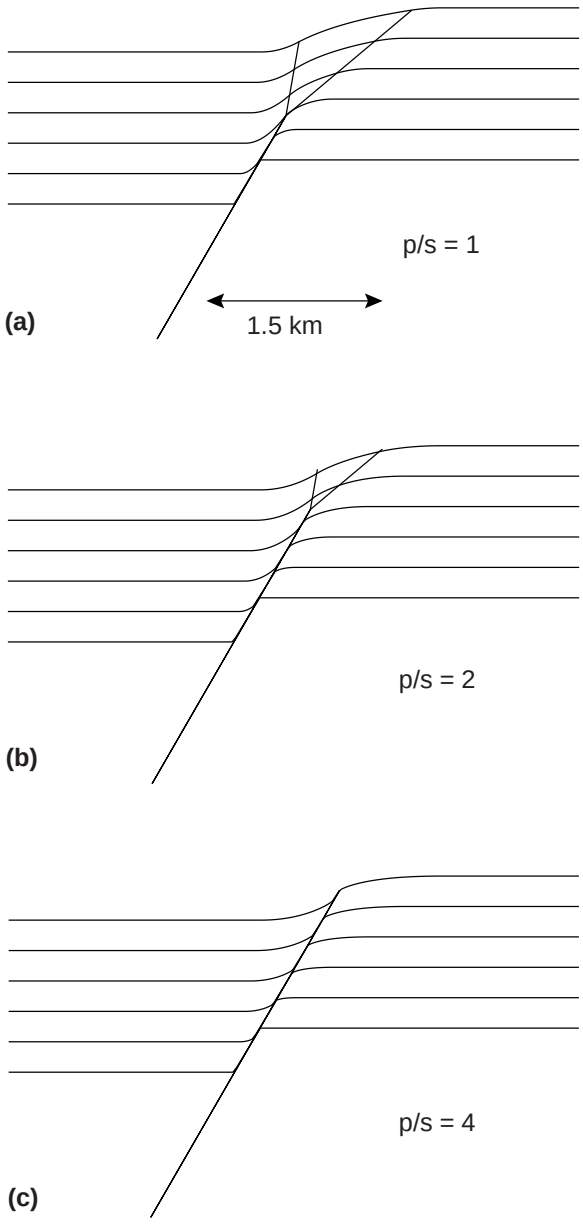

Fig. 5. Model results illustrating the effect of fault propagation to slip (p/s) on fold geometries. Results for p/s ratios of (a) 1.0, (b) 2.0 and (c) 4.0. Total run time is 1 Ma. All other model parameters are as in Fig. 3.

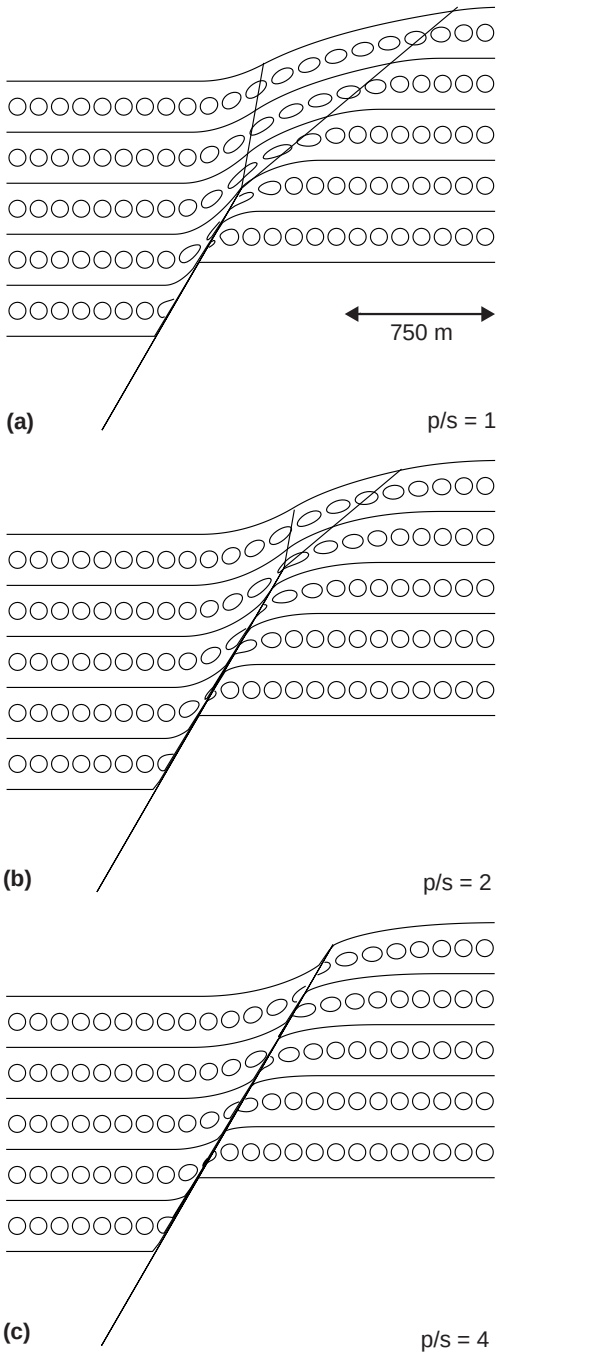

Fig. 6. Distribution and nature of strain in the fault-propagation folds of Fig. 5 illustrated by strain markers. All strain markers were initially circular and had a radius of 50 m.

cement on the normal fault (Fig. 7a). It can be seen that a broad upward-widening zone of distributed deformation develops above the basement fault. Within this zone the primary deformation mechanisms are folding and minor faulting, with both normal faults and high angle reverse faults developed. With increasing displacement the beds above the fault steepen before being cut by the fault. The fault propagates and links upwards such that after 3 cm of displacement the fold is cut by a throughgoing fault which terminates the development of the fold.

The well-constrained nature of this experiment allows the calibration of our kinematic model. From the published data we observe that an apical angle of 80° for the trishear zone approximates well the geometry of the zone of distributed deformation. Therefore there remains only one other parameter to be estimated—the propagation to slip ratio, which, from qualitative inspection (Fig. 7a), can be seen to be in the range from 1.0 to 2.0. It was found that the best fit model required a p/s ratio of 1.5. This model and the

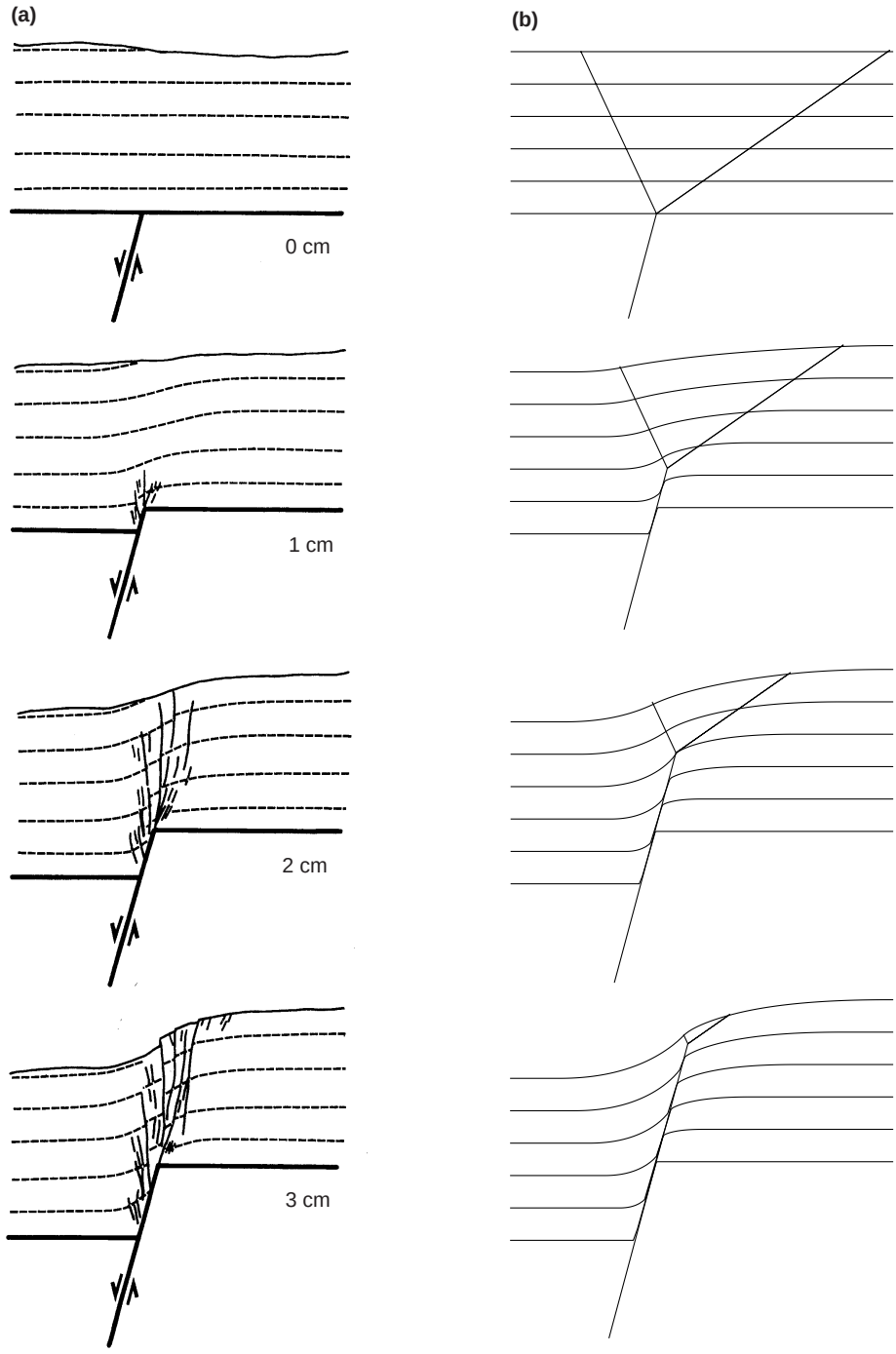

Fig. 7. Comparison of clay analogue modelling results of Withjack et al. (1990) to a model simulation. (a) Analogue model shown after 1, 2 and 3 cm displacement on 75° normal fault. (b) Kinematic model with an apical angle of 80° and a p/s of 1.5 shown at equivalent stages of evolution.

analogue results at equivalent stages of development are shown in Fig. 7(a and b). The close match between the observed and simulated evolution of the structure is remarkable. Many of the details of the structure are accurately reproduced. In particular, the evolution of the monocline and the paired hanging wall-synclines and footwall-anticlines that develop adjacent to the fault are very similar to those seen in the analogue model. In addition, the spatial distribution of folding in both the hanging wall and footwall are reproduced well. Clearly the model does not reproduce the small-scale faulting observed in the clay but the close match between the simulation and the results of Withjack et al. (1990) is very encouraging.

5. Discussion

The model presented here does not attempt to reproduce in detail the outcrop scale features seen in extensional fault-propagation folds. However, it does attempt to predict the broad-scale features and basic characteristics of distributed deformation developed above discrete faults at depth. At this scale, it reproduces well many of the features seen both in analogue models and reported from outcrop and seismic studies (Withjack et al., 1990; Stewart et al., 1996; Gawthorpe et al., 1997). In particular, the model successfully reproduces an upward-widening monocline (fault-propagation fold) linked to a discrete fault at depth. In addition, the model produces hanging wall-synclines and footwall-anticlines adjacent to fault planes that represent breached monoclines rather than drag against the fault plane (cf. Fig. 1c). Field studies indicate that the deformation predicted by the kinematic model is accommodated at the outcrop scale by a variety of mechanisms including ductile flow, bedding slip, rigid rotation and small extensional and thrust faults. While the model does not predict these features, it does predict the spatial variation of strain within a forced fold and the influence of shear zone geometry and fault propagation rate upon both fold style and strain intensity.

While our initial modelling of the analogue model of Withjack et al. (1990) has proved successful, a more rigorous approach to such modelling is needed to quantitatively assess the goodness of fit between the numerical and analogue models. Allmendinger (1998) has recently published an inverse trishear algorithm which allows much more objective calibration of both apical angle and p/s for just such purposes.

Modelling the mechanical controls on the nature of the shear zone, in particular its width, is beyond the scope of this paper. However, Withjack et al. (1990) reported that in their modelling experiments dip of the basement fault exerted a strong control on the width of the zone of distributed deformation, with steeper faults producing narrower zones of deformation. In the kinematic model used here, the fault bisects the apical angle of the shear zone, whilst in experimental results this is only approximately the case (cf. Fig. 1a and b). The relationship between the shear zone orientation and fault dip, together with p/s of the fault, may depend on factors such as the strength of the cover stratigraphy, strain rate, etc. The precise linkage between these mechanical factors and our kinematic model remain to be further investigated.

In many ways the two-dimensional models presented here can also be thought of as representing different stages in the along-strike evolution of a laterally propagating normal fault. Recent authors have noted that discrete (surface-breaking) normal faults often die out along strike into monoclines (Gawthorpe et al., 1997). We suggest that the temporal evolution of our two-dimensional cross-sections could also represent a snapshot in the along-strike development of a propagating normal fault. This has important implications for both the nature and amount of accommodation space developed in the hanging wall of a normal fault. Finally, in this short paper we have concentrated upon the structures seen in strata laid down before deformation began. Growth strata, when present (e.g. Gawthorpe et al., 1997), allow further constraints to be placed upon the evolution of extensional fault-propagation folds. The addition of growth strata to the kinematic model described herein is a straightforward task and is the subject of ongoing work.

6. Conclusions

A two-dimensional kinematic model of extensional fault-propagation folding, based upon trishear, has been presented in this paper. The model links distributed deformation (in a triangular shear zone) ahead of a propagating fault tip to discrete faulting at depth. Key parameters of the model are the apical angle of the shear zone and the fault-propagation to slip (p/s) ratio. The kinematic model reproduces well many of the features seen both in analogue models and reported from outcrop and seismic studies (Withjack et al., 1990; Stewart et al., 1996; Gawthorpe et al., 1997). In particular the model successfully reproduces an upward-widening monocline (fault-propagation fold) linked to a discrete fault at depth. In addition, the model predicts hanging wall-synclines and footwall-anticlines adjacent to the fault plane which represent a breached monocline rather than drag against the fault plane. The model also successfully reproduces the detailed evolution of a clay analogue modelling experiment.

Acknowledgements

This short paper has benefited greatly from discussions with many colleagues, in particular Mary Ford, Rob Gawthorpe, Ian Sharp, John Suppe, Gregg Erickson and Tim Dooley. Reviews by Eric Erslev and Mark Rowan have greatly improved the scope and presentation of the manuscript. A special thanks must go to Rick Allmendinger for his open exchange of ideas and code on trishear kinematics. The first author started this work while part of the Princeton Structure Group whose support is gratefully acknowledged.

References

Allmendinger, R.W., 1998. Inverse and forward numerical modelling of trishear fault-propagation folds. Tectonics 17, 640–656.

Erslev, E.A., 1991. Trishear fault-propagation folding. Geology 19, 617–620.

Gawthorpe, R.L., Sharp, I., Underhill, J.R., Gupta, S., 1997. Linked sequence stratigraphic and structural evolution of propagating normal faults. Geology 25, 795–798.

Hardy, S., Ford, M., 1997. Numerical modeling of trishear fault-propagation folding. Tectonics 16, 841–854.

Janecke, S.U., Vandenburg, C.J., Blankenau, J.J., 1998. Geometry, mechanisms, and significance of extensional folds from examples in the Rocky Mountain Basin and Range province, U.S.A. Journal of Structural Geology 20, 841–856.

Laubscher, H.P., 1982. Die Sudostecke des Rheingrabens—ein kinematisches und dynamisches problem. Eclogae Geologicae Helvetiae 75, 101–116.

Patton, T.L., Fletcher, R.C., 1995. Mathematical block-motion model for deformation of a layer above a buried fault of arbitrary dip and sense of slip. Journal of Structural Geology 17, 1455–1472.

Schlische, R.W., 1995. Geometry and origin of fault-related folds in extensional settings. American Association of Petroleum Geologists Bulletin 79, 1661–1678.

Stewart, S.A., Harvey, M.J., Otto, S.C., Weston, P.J., 1996. Influence of salt on fault geometry: examples from the UK salt basins. In: Alsop, G.I., Blundell, D.J., Davison, I. (Eds.), Salt Tectonics, 100. Geological Society Special Publication, pp. 175–202.

Withjack, M.O., Meisling, K.E., Russell, L.R., 1988. Forced folding and basement-detached normal faulting in the Haltenbanken area, offshore Norway. American Association of Petroleum Geologists Bulletin 72, 259.

Withjack, M.O., Olson, J., Peterson, E., 1990. Experimental models of extensional forced folds. American Association of Petroleum Geologists Bulletin 74, 1038–1045.